FOREX Publication
Open Access | Rapid and quality publishing

International Journal of
Electrical and Electronics Research (IJEER)
Research Article | Volume 12, Issue 1 | Pages 178-186 | e-ISSN: 2347-470X

Wind Energy Conversion System using Cascading H-Bridge Multilevel Inverter in High Ripple Scenario

Chellam S [1], Kuruseelan S[2] and Jasmine Gnanamalar A[3]
[1]*Department of Electrical and Electronics Engineering, Velammal College of Engineering and Technology, Madurai, Tamil Nadu, 625 009 India, scv@vcet.ac.in*
[2]*School of Electrical Engineering, Vellore Institute of Technology, Chennai, Tamil Nadu 600 127 India; kuruelectrix@gmail.com*
[3]*Department of Electrical and Electronics Engineering, PSN College of Engineering and Technology, Tirunelveli. India, jasmine@psncet.ac.in*

***Correspondence:** Chellam S; scv@vcet.ac.in

ABSTRACT- This paper presents wind energy conversion system using CHB MLI and phase interleaved boost converter to overcome high voltage and current ripple. Developments in power electronics technology have a direct impact on advances in wind energy conversion systems. WECS output voltage may fluctuate depending on wind speed. For WECS to maintain a constant output voltage, a power converter is required. This paper explains how to configure a phase-interleaved boost converter and voltage controller to maintain a stable intermediate circuit voltage in the system. The proposed cascading H-bridge multilevel inverter (CHB MLI) converts DC/AC using a novel topology. Separate DC sources are not utilizing the suggested topology. Multi-level inverters are operated by specific harmonic disposal pulse width modulation, or SHE-PWM are utilized. PMSG voltage, CHB-MLI voltage, boost converter voltage and rotor speed have seven different levels of simulated waveforms. Among the many advantages of three-phase alternating DC-DC boost converters, that are high efficiency, fast dynamics and very low current ripple. The output voltage is increased to 400 V using a three-phase interleaving converter, which also maintains a higher efficiency of about 98%. DC-DC power converters have proven to be essential components of many applications and topologies. The interleaving technique is necessary to address the main disadvantages of DC-DC power converters: increased voltage, reduced efficiency, and rippled current. Interleaved boost converters have several advantages, including lower switching losses, lower voltage and current ripple, increased efficiency, and more. To improve the converter's overall functionality, the "n" parallel converter is connected through an interleaved boost converter. This paper presents a performance analysis of a multiphase alternating boost converter to reduce high voltage and current ripple. MATLAB/Simulink is used for analysis and simulation of phase-interleaved boost converters.

Keywords: Phase Interleaved Boost Converter; DOF-PID Controller; Wind Energy Conversion System; Cascaded H-Bridge Inverter.

ARTICLE INFORMATION
Author(s): Chellam S, Kuruseelan S and Jasmine Gnanamalar A
Received: 08/12/2023; **Accepted**: 20/02/2024; **Published**: 15/03/2024;
e-ISSN: 2347-470X;
Paper Id: IJEER 0812-06;
Citation: 10.37391/IJEER.120126
Webpage-link:
https://ijeer.forexjournal.co.in/archive/volume-12/ijeer-120126.html

Publisher's Note: FOREX Publication stays neutral with regard to Jurisdictional claims in Published maps and institutional affiliations.

1. INTRODUCTION

The main goal of a DC-DC converter is to raise the input voltage to the appropriate output voltage level and achieve significant voltage gain [1]. The converter's duty cycle needs to be higher than 50% in order to produce the necessary voltage level. An interlacing boost converter for regenerative systems is proposed as a solution to this problem. Interleaved boost designs are becoming an increasingly effective tool for efficiently managing input current as power density increases. Step-up converters operating in two phases are used in applications requiring high efficiency, low current ripple, fast dynamics, and increased power density. The inductance current of an interleaving boost converter can be reduced by using interleaving technique [2]. The output current of the capacitor will have significant ripple if a simple conventional boost converter is used, and the current supplied to the load will be random. The need for low input voltage and high voltage gain is especially evident in expanding automotive power conversion application fields [3].

DC/DC converters with multiple levels are regarded as a substitute that satisfies requirements like high power density and low blocking voltage. [4-6]. Compared with the conventional topology proposed in [7], a multilevel resonant FC converter with symmetrical structure and fewer active switching devices was introduced in [6]. Therefore, the equivalent series resistance of each part in the circuit can affect the resonance frequency of each charge/discharge loop. As a result, each resonant frequency will oscillate above or below a specific switching frequency.

The largest and most complex multilevel topology is arguably the general multilevel topology presented in [8]. In this topology, the clamping components can be active switches or passive devices (capacitors and diodes). Its abundance of passive components and active switches is its main disadvantage, making it difficult to commercialize in

FOREX Publication
Open Access | Rapid and quality publishing
International Journal of Electrical and Electronics Research (IJEER)
Research Article | Volume 12, Issue 1 | Pages 178-186 | e-ISSN: 2347-470X

application in real life. Based on the multilevel modular inverter, a modular DC/DC converter with multiple levels has been suggested in [9, 10] due to its many advantages, including low EMI, fast transient response, power distribution, small passive component size (especially for output filters), and low current ripple.

Because of the uniform distribution of high input current between parallel components in this circuit configuration, there are fewer current stresses the semiconductor devices and lowering losses. Furthermore, the continuous conduction mode interleaving approach improves the DC-DC boost converter's performance and dependability by mitigating the control impact of input current and output voltage.

The paper's contribution is that due to the inherent limitation of wind power, the wind turbine's output voltage must be increased in slow wind conditions.

- The voltage multiplier and interleaved three-phase boost converter produce a better voltage gain and less output and input current ripple when compared to traditional boost converters.
- Additionally, the converter is only capable of handling half the output voltage at its voltage limit. However, if the converter operates with a light load, the switches will receive a higher voltage.
- The problem of higher voltage stress at light loads is resolved by the new PWM control scheme.
- To keep low voltage difficulties on the power range switches, the traditional alternating PWM technique is coupled with the suggested PWM control mechanism at higher loads.
- In the end, the experiment confirms the control scheme. Low wind conditions increase the output voltage of a PMSG and decreases in high wind conditions, remaining constant through the DOF PID controller.

The following research illustrate the remaining section of this study. *In Section 2*, related work is explained. The suggested approach and the related algorithm are described in *Section 3*. *Section 4* analyses the results of the implementation. *Section 5* presents conclusions and next steps.

2. RELATED WORK

M. A. Harimon et al. (2017) [11] proposed, a three-phase AC DC-DC boost converter can increase the DC output voltage when the input voltage and current are low by reducing the ripple in the output voltage and input current, the interleaving technique with continuous conduction improves the efficiency as well as the suggested techniques' accuracy.

K. Latha Shenoy et al. (2017) [12] presents the planning, construction and evaluation of interleaved boost converters for use in green energy projects. An output voltage of 400 V can be generated from an input voltage of 100 V using the interleaving technique. This is done in an open loop framework. Through the system, transmit the power to the load more efficiently. The efficiency obtained by this method is 98%.

Prachi Shinde et al. (2018) [13] proposed a traditional interleaved boost converter with an interleaved structure to lower the input curve and input voltage ripple. Increased efficiency is achieved by using capacitive and inductive switching.

S. Kirubadevi et al. (2022) [14] proposed wind power system using permanent magnets and synchronous generators is considered for analysis. Wind energy conversion efficiency can be increased by improving electronic power control circuits and maximum power point tracking (MPPT).

Btissam Majout et al. (2022) [15] provides a precise sliding mode control method that solves the vibration problem with conventional sliding mode control and is built upon a unique method for constant, smooth operation. When using a synchronous generator with permanent magnets and variable wind speed, a control strategy is implemented.

3. PROPOSED WIND ENERGY CONVERSION SYSTEM

In *figure 1*, a three-phase load, PMSG, phase-alternating boost converter, diode bridge rectifier, and applied CHB are shown. The electrical energy from wind energy that the PMSG converts is received by the diode bridge rectifier. To create a closed loop and generate the required voltage for the output, the DC output is rectified and fed into the boost converter. The 3-phase load is powered by a seven-level three-phase CHB inverter, which receives output from the boost converter.

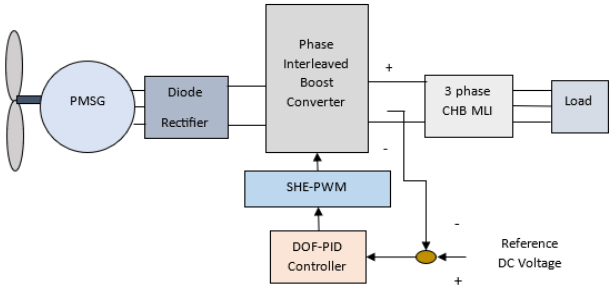

Figure 1: 3-phase PMSG based WECS

3.1 Wind Turbine Modelling

Equation 1 provides the energy extracted from the wind according to a known affinity.

$$P_w = \frac{1}{2} c_p \rho A v_w^3 \quad (1)$$

The wind speed is v_w, the power factor is cp and A= πR^2 is the floating area of the rotor in linear meters and the rotor radius is R. Air density is expressed as ρ, which is 1.225 kg/m3 at 288 K and 1 atmospheric pressure.

The wind turbine's efficiency in converting wind energy into electrical power is measured by its coefficient of power.

$$\text{Coefficient of power} = \frac{\text{power generated by the wind turbine}}{\text{total power in the wind}}$$

FOREX Publication
Open Access | Rapid and quality publishing
International Journal of Electrical and Electronics Research (IJEER)
Research Article | Volume 12, Issue 1 | Pages 178-186 | e-ISSN: 2347-470X

Assuming a ratio λ between bank angle and maximum speed, *equation (2)* gives cp. The c_p function, which is depending depending on the pitch angle γ and tip speed λ.

$$c_p(\lambda,\gamma) = c_1(c_2\frac{1}{\beta} - c_3\gamma - c_4\gamma^x - c_5)e^{-c_6\frac{1}{\beta}} \quad (2)$$

The turbine's dimensions and type determine the coefficients c1 through c6, and x. The power coefficient selected by the wind turbine, C_p, β is determined by a function of λ and γ is provided by *eqn. (3).*

The x- type and size of the turbine determine the coefficients c_1 to c_6, β which are functions of λ and γ, given by *equation (3).*

$$\frac{1}{\beta} = \frac{1}{\lambda+0.08\gamma} - \frac{0.035}{1+\gamma^3} \quad (3)$$

A wind turbine is used to generate mechanical energy by converting kinetic energy of the wind into mechanical energy. This section examines HAWT because of its excellent efficacy. Furthermore, the following indicates the machine tip-speed ratio (λ):

$$\text{Where } \lambda = \frac{\omega_w R}{v_w} \quad (4)$$

Here λ is the machine tip-speed ratio. The variables R represent the blade length, ω_w - rotor speed (in rad/s), and wind speed (in m/s) - v_w, respectively.

Every wind turbine uses aerodynamic forces to capture wind energy. The two primary forces in aerodynamics are lift and drag. Lift acts perpendicular to the relative flow, whereas drag pushes the body in that direction.

Equation. (5) gives the aerodynamic torque (τ_w) in Nm.

$$\tau_w = \frac{P_w}{\omega_w} \quad (5)$$

where rotor speed (ω_w) is expressed in rad/s and P_w is a mechanical power. Because there is no gearbox, the aerodynamic and mechanical moments of the generator are equal.

3.2 PMSG Modelling

With PMSG, wind turbines can operate at variable speeds. There are many benefits to using PMSG, including fewer maintenance issues due to the absence of excitation and slip rings. It is cheaper because it does not require a gearbox when used to convert wind energy. The dq model of the PMSG, based on a synchronously rotating reference frame, is given by *equations (6) to (13).*

$$v_q^r = R_s i_q^r + \omega_r \psi_d^r + p\psi_q^r \quad (6)$$

$$v_d^r = R_s i_d^r + \omega_r \psi_q^r + p\psi_d^r \quad (7)$$

Where Rs is the stator resistance per phase, the flux connection on the d and q axes is represented by, $i_q^r$and i_d^r rare and p=d/dt respectively. The q and d-axis voltages are expressed as v_q^r and v_d^r. The q and d axis flow links are described as $\psi_q^r = L_q i_q^r$, $\psi_d^r = L_d i_d^r + \psi_{pm}^r$

where ψ_{pm}^r is the permanent magnet flux linkage, and the corresponding L_d and L_q. With the above substitutions made *eqns. (6) and (7)* become

Where the permanent magnet flux linkage is ψ_{pm}^r and L_d and L_q are the stator's d- and q-axis inductances. respectively.

When the above is substituted, *eq. (6) and (7)* become

$$v_q^r = R_s i_q^r + \omega_r (L_d^r i_d^r + \psi_{pm}^r) + pL_q^r i_q^r \quad (8)$$

$$v_d^r = R_s i_d^r - \omega_r L_q^r i_q^r + p(L_d^r i_d^r + \psi_{pm}^r) \quad (9)$$

Since $p\psi_{pm} = 0$,

$$v_d^r = R_s i_d^r - \omega_r L_q^r i_q^r + pL_d^r i_d^r \quad (10)$$

The PMSG moment equation is given by *equation (11).*

$$T_e = \left(\frac{3}{2}\right)\left(\frac{P}{2}\right)\left(\psi_d^r i_q^r - \psi_d^r i_q^r\right) \quad (11)$$

Equations (12) and (13) provide formulas for calculating active and reactive power.

$$P = \frac{3}{2}(v_d^r i_d^r + v_q^r i_q^r) \quad (12)$$

$$Q = \frac{3}{2}(v_q^r i_d^r + v_d^r i_q^r) \quad (13)$$

3.3 Diode Bridge Rectifier

The PMSG's three-phase AC voltage is converted to DC voltage using a diode rectifier. On the other hand, a rectifier's average output voltage can be obtained by applying *equation (14).*

$$V_{oavg} = \frac{3\sqrt{3}V_{mph}}{\pi} \quad (14)$$

where V_{mph} represents maximum phase voltage of the PMSG.

3.4 DOF PID Controller

The first and most important factor to consider when designing a control system is the degrees of freedom (DOF), determines the viability of system control and corresponds to the maximum number of threads that can be controlled simultaneously.

$$u = K_p(br - y) + \frac{K_i}{s}(r - y) + K_{ds}(cr - y) \quad (15)$$

Figure 2 illustrates the DOF PID control system. Fast output response and lack of stability characterize the four-phase alternating boost converter system. Less stable errors and simpler reaction times are two advantages of DOF PID controllers. For this reason, choosing a DOF PID controller for this system is very suitable.

FOREX Publication
Open Access | Rapid and quality publishing
International Journal of Electrical and Electronics Research (IJEER)
Research Article | Volume 12, Issue 1 | Pages 178-186 | e-ISSN: 2347-470X

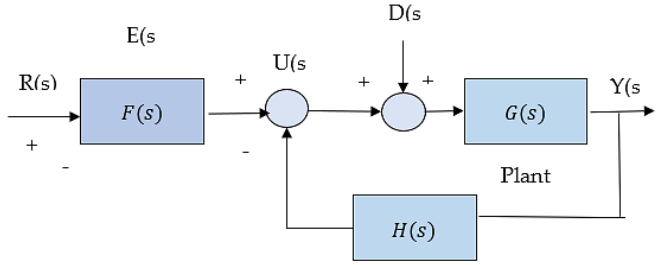

Figure 2: Operation diagram of the DOF PID controller

3.5. Formatting of Mathematical Components

Figure 3 depicts the circuit of a three-phase AC DC-DC boost converter. This circuit layout includes the recommended circuit layout, electricity diodes (D_1, D_2, and D_3) and power switches (S_1, S_2, and S_3) and three step-up inductor equivalents (L_1, L_2 and L_3). The load R and each phase of the converter's output filter capacitor C are linked. At each phase switch, the duty cycle D is constant, but the phase difference is 360 m/n, where the phase function is n. In this configuration, there is a 120° phase shift between each phase.

Three separate boost switches work together to form an interleaving circuit. All stages of the converter will operate like conventional boost converters. Because it offers advantages over discontinuous conduction mode (DCM) and works well with interleaved boost converters, continuous conduction mode (CCM) was chosen. In the initial mode, S_1, S_2, and S_3 are all closed. As for the second, third, fourth and fifth forms, it is identical; in the sixth case, Additionally, both when S_1 is closed and S_2 and S_3 are both open, and when S_2 is closed and S_1 and S_3 are both open as well.

The time variation is (1-D)/T during open time (t-open) and DT during closing time (t-close). The timing diagram for converting signals with a 120° phase difference between signals is shown in *figure 2*.

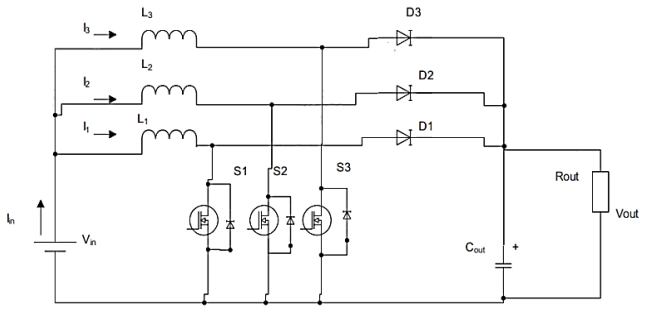

Figure 3: Three-phase interleaved DC-DC boost converter

The circuit of a three-phase AC DC-DC boost converter can be identified by its reduced output voltage ripple and decreased input current voltage. An AC DC-DC boost converter with three phases: its circuit design is characterized by two things: reduced output voltage ripple and reduced input current limitation. The switching signal's time diagram is displayed in *figure 4.*

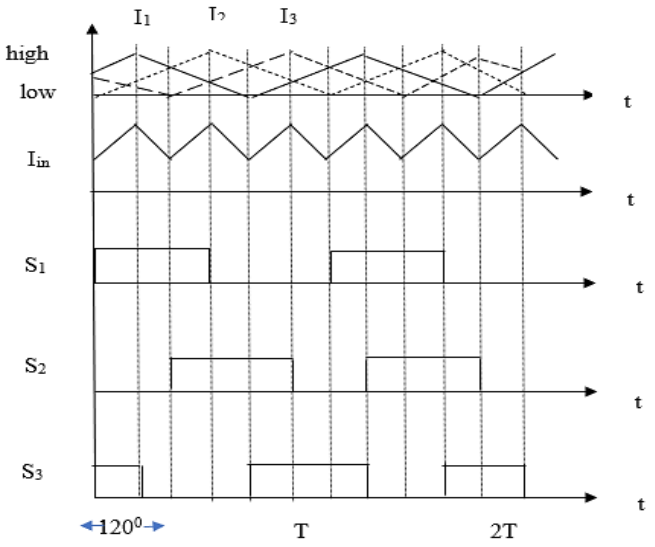

Figure 4: MOSFET gate signal waveform, input current, and phase current (inductance current)

The total current passing through all of the inductors (I_{in}) is the input current of an interposer. One of three parallel phases can then be used to separate the high input current and low input voltage. Accordingly, switching components with lower current values can be considered. In addition, because power switches S_1, S_2 and S_3 have the same duty cycle D, the average value of inductance currents I_1, I_2, and I_3 has a phase shift of 120° and is evenly distributed. The ripple suppression function reduces ripples in the input voltage and output current.

3.6 Proposed CHB Multilevel Inverter

Multi-level inverters (MLIs) are popular because they have fewer EMI problems and possess the ability to deliver high voltage and high power. Compared with traditional inverters, PWM has less total harmonic distortion (THD), switching losses, and three or more voltage levels. As a result, their use in controlling medium and high voltage AC drives has increased [8-9]. Multi-level inverter designs have been created in a variety of ways, including: inverters classified as three different kinds of inverters: flying capacitors, neutral point inverters (NPC), and cascaded H-bridge (CHB) inverters. Among these, clamping diodes and capacitors are not needed for the CHB inverter.

Using a series of cascading single-phase inverter modules, they are capable of reaching high voltages. They need the least number of parts to function. They are also powerful, flexible and easy to control. The disadvantage of CHB inverters is that they require separate DC power. As shown in *figure 2*, a sector of a seven-level CHB is proposed using a single DC source. A transformer connects the load to the inverter output. Three transformers are used in the inverter and a series connection is made between their secondary windings. The connection is made between the load and the secondary winding of the transformer [16-17]. There are seven voltage levels: $\pm V_{DC}$, $2\pm V_{DC}$, $\pm V_{DC}$, 0.

FOREX Publication
Open Access | Rapid and quality publishing
International Journal of Electrical and Electronics Research (IJEER)
Research Article | Volume 12, Issue 1 | Pages 178-186 | e-ISSN: 2347-470X

For conventional inverters, the multicarrier sinusoidal PWM method is used control method [18-19]. Its popularity comes from its ease of use and the beneficial effects it generates first harmonics under all operating conditions, including the "overmodulation" that allows them [20-23]. It is very simple to use and can be applied to any MLI. An m-1 carrier or a triangle wave of the same frequency and amplitude is required for m-class inverters [24-26]. CHB Inverter with Seven Levels and One DC Source is shown in *figure 5*.

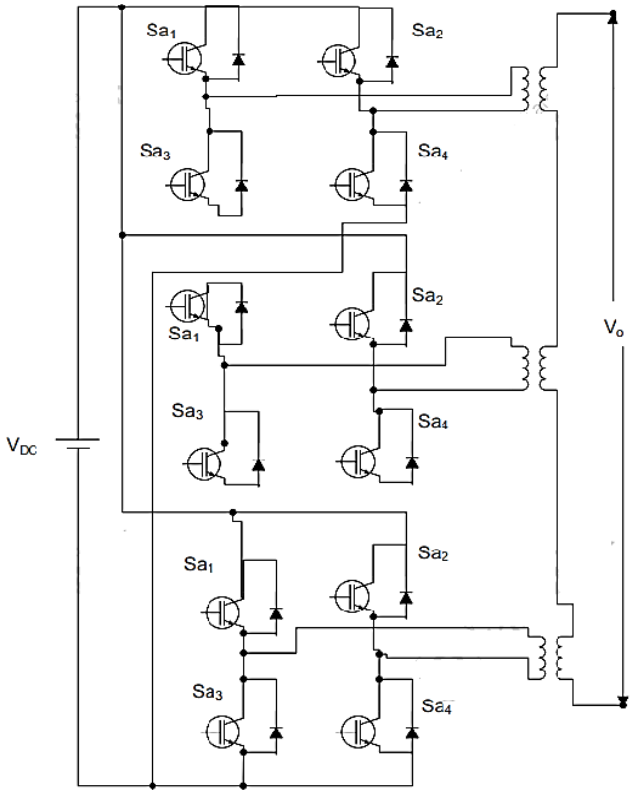

Figure 5: CHB Inverter with Seven Levels and One DC Source

The most widely used control method for traditional inverters is known as multicarrier sinusoidal PWM, or simply multicarrier sinusoidal PWM. It is simple to deploy and works with any MLI. An m-1 (triangular) carrier wave of the same amplitude and frequency is required for the m-level inverter [27-30].

The following four carrier pulse control strategies have distinct phase relationships:

- Phase arrangement (PD) uses (m–1) carriers, all in phase with each other. Six carriers are compared with one sine wave for a seven-level inverter. With vertical displacement, the six carriers are grouped together.
- The carrier (m-1) is used in a phase difference (POD) arrangement, where all operators are 180 degrees out of phase and in phase with the carriers above and below ZERO reference. There is a vertical variation in the arrangement of the six carriers.
- Each carrier wave in an alternating phase opposition pattern (APOD) is offset 180 degrees from the next and is compensated vertically (m-1).
- Phase shifting (PS) uses carrier waves (m-1), each shifted by $2\pi/(m-1)$ radians. The specified CHB inverter switching signals can be generated using PID technique. When comparing the sinusoidal modulated signal with six triangular carriers, a control signal is generated. Since the PID scheme gives the least harmonic distortion to the line voltage.

4. SIMULATION AND RESULTS

Different wind speeds are simulated for the system using MATLAB/Simulink. The line, phase, boost converter, rotor speed, and voltage waveforms of the PMSG's CHB-MLI are represented by the simulated waveforms in *figures 6-10*. The phase "*a*" voltage of the PMSG is shown in *figure 7*. Voltage fluctuates. as a function of the rotor speed of the PMSG at times t = 2s, 5 s, and 8.5 s PMSG, wind, as shown in *figure 6* and *figure 7*.

The PMSG voltage change resulting in the boost converter voltage change at 2.5, 5, and 7.5 seconds is shown in *figure 8*. Then it takes 3.5, 5.7 and 9 seconds respectively to reach the reference DC voltage of 225 V.

Additionally, the PLC's phase and line voltage varied at 2.5, 5, and 7.5 seconds, respectively, before stabilizing at 3.5, 5.7, and 9 seconds. *Figures 9 and 10* depict the PLC's line voltage and phase on an enlarged scale. The phase voltage of the PLC is shown in *figure 11* at an enlarged scale.

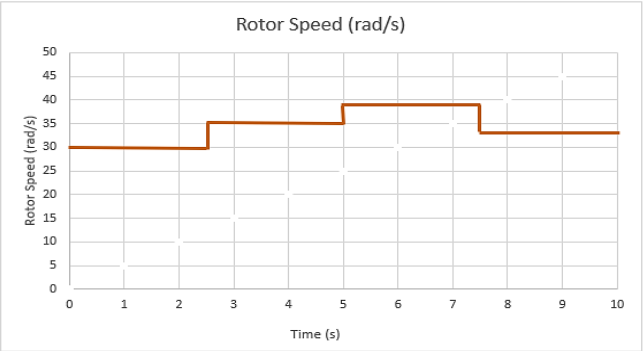

Figure 6: Rotor speed of the PMSG

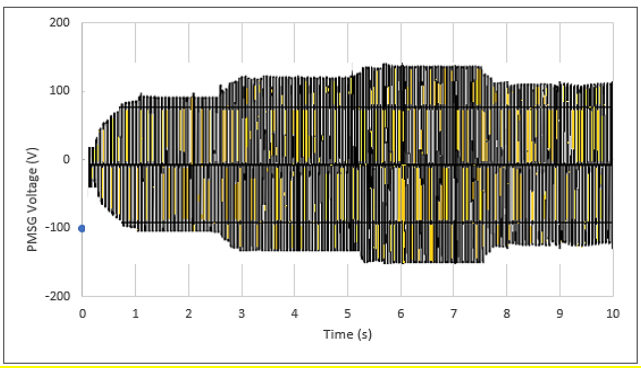

Figure 7: Phase 'a' voltage of the PMSG

FOREX Publication
Open Access | Rapid and quality publishing
International Journal of Electrical and Electronics Research (IJEER)
Research Article | Volume 12, Issue 1 | Pages 178-186 | e-ISSN: 2347-470X

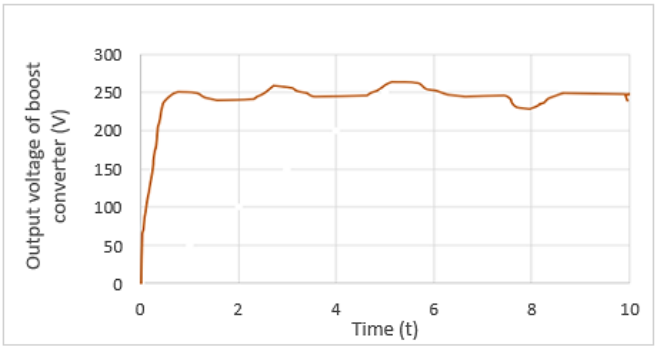

Figure 8: Boost converter voltage

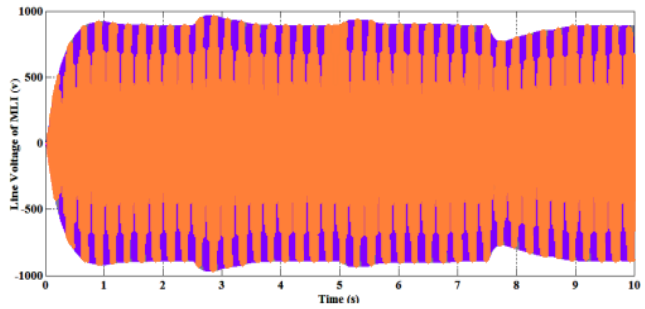

Figure 9: Line Voltage of the MLI

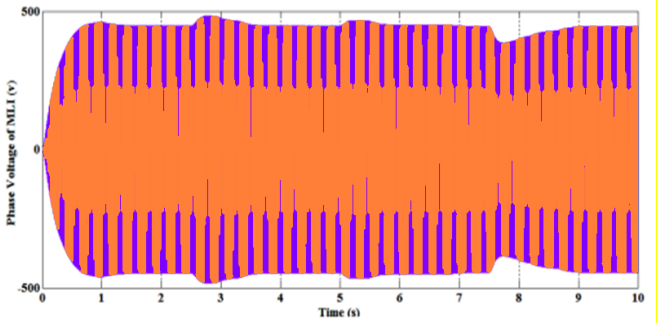

Figure 10: Phase voltages of the MLI

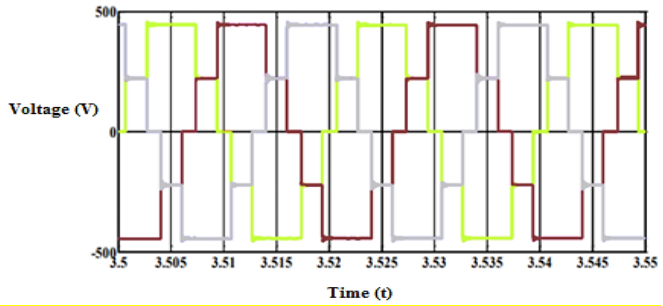

Figure 11: MLI extended range phase voltage

The simulation and experimental parameters for the three-phase DC-DC boost converter and the conventional DC-DC boost converter are shown in *table 1*. *Table 2* shows the Parameters and its units used in the proposed system.

Table 1: Specifications

Specification	Value
Inductance L (mH)	25
Power, P (W)	25
Boost Ratio, β	2
Load Resistance, R (Ω)	100
Output Ripple, r (%)	1
Inductance (interleaved), L_1, L_2, L_3 (mH)	1
Input voltage/Output voltage, Vin /Vo (V)	25/50
Capacitance, C (μF)	470
Duty Cycle, D	0.5
Switching Frequency, f (kHz) 25	25

In this analysis, the specifications of both converters are the same. Based on the simulation results, *figures 12 and 13* depict the fluctuations in the three-phase AC DC-DC boost converter's output voltage and input current, respectively. As shown in *figures 13* and *14*, the interleaving converter's input current (Iin) is the total current passing through all of the inductors. The high input voltage and low input current can then be separated using one of the three parallel phases. Therefore, it has been demonstrated that the three-phase alternating DC-DC boost converter connection significantly reduces input as well as output current, voltage ripple.

Table 2: Parameters and its units used in the proposed system

Variables	Description	Units
Rated power	1.5	MW
Blade radius, R	35.25	m
Rotor speed	*120–210*	*m/s*
Resistive Load	20	kW
Load resistance	6.5	Ω
Capacitor link	5000	uF
Load voltage	360	Volts
Boost converter voltage	250	Volts
Line Voltage of the MLI	560	Volts
Phase voltages of the MLI	490	Volts
Output voltage of DC-DC boost converter	0.92	meter
Output current of DC-DC boost converter	49.99	meter

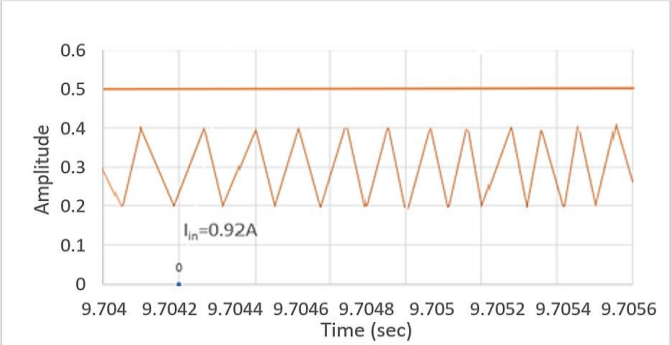

Figure 12: Output current ripple for the 3-ϕ interleaved DC-DC boost converter

FOREX Publication
Open Access | Rapid and quality publishing
International Journal of Electrical and Electronics Research (IJEER)
Research Article | Volume 12, Issue 1 | Pages 178-186 | e-ISSN: 2347-470X

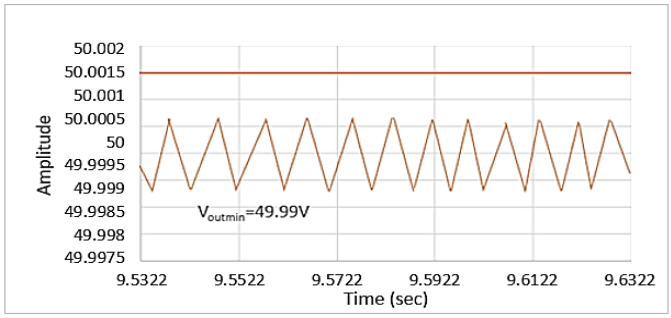

Figure 13: Output voltage ripple simulation results for 3-ϕ alternating DC-DC boost converter

Therefore, it also reduces the conduction loss of semiconductor devices. *Figure 15* illustrates the current limit of a three-phase AC DC-DC boost converter on a semiconductor. The current limit has been shown to decrease with increasing stage frequency in an AC boost converter.

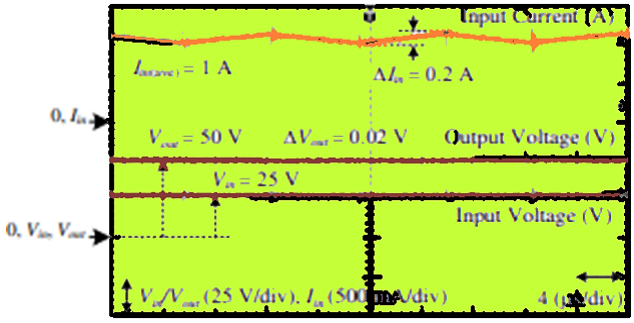

Figure 14: Three-phase AC DC-DC step-up converter experimental results: measured input voltages, output voltages and input currents

Three-phase DC-DC. Therefore, it is widely accepted that considering the use of multiphase DC-DC boost converters will help reduce the conduction losses of semiconductor devices and limit the low-voltage current. The converter performs better overall and is therefore more reliable. The waveform of the three-phase interleaved DC-DC boost converter illustrates the stress on semiconductors in *figure 15*.

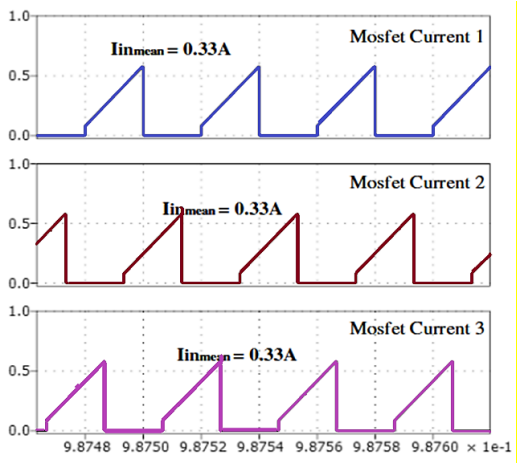

Figure 15: Stress on semiconductors in the three-phase interleaved DC-DC boost converter

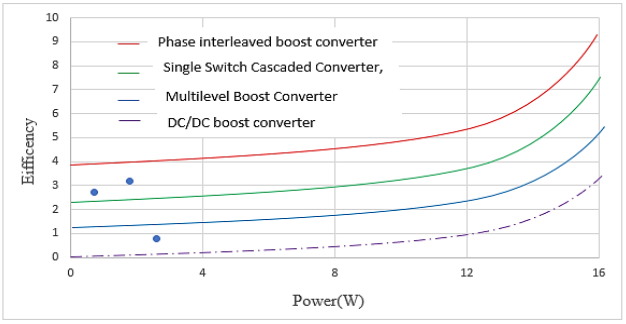

Figure 16: Voltage gain between the existing converter and the proposed converter

The recommended converter's performance is displayed in *figure 16* and experimentally measured under load. The power and efficiency are measured at different loads by varying the load resistance. At 16 watts rated power, efficiency is 91.3% and efficiency reaches a maximum of 92.5%, Increasing conduction losses reduces efficiency to 87.7%.

5. CONCLUSIONS

The implementation of a phase alternating boost converter and a voltage controller capable of maintaining a stable intermediate circuit voltage in the system will be discussed. The voltage is regulated by a boost converter in reaction to variations in wind speed. The voltage controller attains the responsibility of maintaining a constant DC output voltage to the boost converter. The CHB-MLI topology needs to be reconsidered to eliminate the need for a separate DC power supply. SHEPWM is used to enable MLI. Simulated waveforms have been obtained for PMSG rotor speed, voltage, pulse signal gain, line voltage, and phase angle. The waveforms convincingly demonstrate that the designed PI controller and boost converter can maintain the DC voltage at an appropriate level. This article has covered several areas related to three-phase AC DC-DC step-up converters.

According to the findings, when cascaded H-bridge inverters are utilized with WECS, they result in lower THD. Using the nearest level modulation technique, this cascaded topology is compared to the Modular Multilevel Converter (MMC) and it is found that MMC performs better than cascaded H-bridge inverters since its THD is almost half that of the latter. Consequently, there will be less system cost. A modular multilevel converter may process high voltages without the need to connect series-switching components. By supplying high-quality power and lowering common-mode voltages, they can accomplish greater amounts of output levels with increased efficiency and fewer harmonic content.

Compared with existing boost converters, the voltage multiplier and interleaved three-phase boost converter result in decreased input and output current ripple and increased voltage gain. Additionally, the converter is only capable of handling half the output voltage at its voltage limit. However, if the converter operates with a light load, the switches will receive a higher voltage. The problem of higher voltage stress at light loads is addressed by the new PWM control architecture. The

International Journal of
Electrical and Electronics Research (IJEER)
Research Article | Volume 12, Issue 1 | Pages 178-186 | e-ISSN: 2347-470X

experiment confirms the control scheme were the low wind conditions increase the output voltage of a PMSG and decreases in high wind conditions. The analysis shows that current stress is reduced by 33% and semiconductor conduction loss is reduced by 32%. Additionally, this helps reduce semiconductor conduction losses in the converter due to the alternating multi-phase configuration. The voltage across the switches of the suggested converter is 60% lower than that of a traditional interleaved boost converter.

The following is the project's future scope.

A. By employing this method and utilizing advanced power electronics equipment, we can lower harmonics in the output waveform while raising the inverter's level.
B. The HVDC power transmission and electric car drives will be another area in which this approach is used.
C. Power electronics devices provide high speed and a significant amount of automation.

Author Contributions: The authors confirm contribution to the paper as follows: study conception and design: Chellam. S, Kuruseelan. S; data collection: Jasmine Gnanamalar. A; analysis and interpretation of results: Chellam. S; draft manuscript preparation: Kuruseelan S. G All authors reviewed the results and approved the final version of the manuscript.

Acknowledgments: The author would like to express his heartfelt gratitude to the supervisor for his guidance and unwavering support during this research for his guidance and support.

Conflicts of Interest: Regarding the current research, the authors have stated that there are no potential conflicts of interest that should be reported by them.

REFERENCES

[1] Swamy, H. M.; Guruswamy, K. P.; Singh, S. P. Design, Modeling and Analysis of Two-Level Interleaved Boost Converter. IEEE International Conference on Machine Intelligence and Research Advancement (ICMIRA) 2013, pp. 509-514.

[2] Ghosh, A.; Banerjee, S.; Sarkar, M. K.; Dutta, P. Design and Implementation of Type-II and Type-III Controller for DC-DC Switched-Mode Boost Converter by using K-Factor Approach and Optimization Techniques. IET Power Electronics 2016, Volume 9, No 5, pp. 938-950.

[3] Shin, H. B.; Park, J. G.; Chung, S. K.; Lee, H. W.; Lipo, T. A. Generalised Steady-State Analysis of Multiphase Interleaved Boost Converter with Coupled Inductors. IEE Proc. Electr. Power Appl 2005, Volume 152, No 3, pp.584–594.

[4] Cao, D.; Peng, F. Z. Zero-current-switching multilevel modular switched-capacitor DC–DC converter. IEEE Trans. Ind. Appl. 2010, Volume 46, No 6, pp. 2536–2544.

[5] Qian, W.; Cao, D.; Cintro-Rivera, J. G.; Gebben, M.; Wey, D.; Peng, F. Z. A switched-capacitor DC–DC converter with high voltage gain and reduced component rating and count. IEEE Trans. Ind. Appl. 2012, Volume 48, No4, pp.1397-1406.

[6] Parastar, A.; Gandomkar, A.; Seok, J. K. High efficiency multilevel flying-capacitor DC/DC converter for distributed renewable energy systems. IEEE Trans. Ind. Electron 2015, Volume 62, No 12, pp. 7620-7630.

[7] Zhang, F.; Du, L.; Peng, F. Z.; Qian, Z. A new design method for high-power high-efficiency switched-capacitor DC–DC converters. IEEE Trans. Power Electron 2008, Volume 23, No 2, pp. 832-840.

[8] Peng, F. Z.; A generalized multilevel inverter topology with self-voltage balancing. IEEE Trans. Ind. Appl 2001, Volume 37, No 2, pp. 611–618.

[9] Kish, G. J.; Ranjram, M.; Lehman, P. W. A modular multilevel DC/DC converter with fault blocking capability for HVDC interconnects. IEEE Trans. Power Electron 2015, Volume 30, No 1, pp. 148– 161.

[10] Ferreira, B.; The multilevel modular DC converter. IEEE Trans. Power Electron 2014, Volume 28, No 10, pp. 4460–4465.

[11] Harimon, M. A.; Ponniran, A.; Kasiran, A. N.; Hamzah, H. H. A study on 3-phase interleaved DC-DC boost converter structure and operation for input current stress reduction. Int. J. Power Electron. Drive 2017, Volume 8, No 4, pp.1948-1953.

[12] Shenoy, K. L.; Nayak, C. G.; Mandi, R. P.; Design and implementation of interleaved boost converter. International Journal of Engineering and Technology (IJET) 2017, Volume 9, No 3S, pp.496-502.

[13] Shinde, P.; Narvekar, P.; Manik Kumbhar, M. Three Phase Interleaved Boost Converter. International Research Journal of Engineering and Technology (IRJET) 2018, Volume 5.

[14] Kirubadevi, S.; Sutha, S. PMSG Based Wind Energy Conversion System Using Intelligent MPPT with HGRSC Converter. Intelligent Automation & Soft Computing 2022, Volume 34, No. 2.

[15] Majout, B.; Bossoufi, B.; Bouderbala, M.; Masud, M.; Al-Amri, J. F.; Taoussi, M.; Karim, M. Improvement of PMSG-based wind energy conversion system using developed sliding mode control. Energies 2022, Volume 15, No 5, pp.1625.

[16] Urmila, B.; Subbarayudu, D. Multi-level Inverter: A Comparative Study of Pulse Width Modulation Techniques. International Journal of Scientific and Engineering Research 2010, Volume 1, No 3, pp. 2-5.

[17] Colak, I.; Kabalci, E.; Bayindir, R. Review of multilevel voltage source inverter topologies and control schemes. Energy conversion and management 2011, Volume 52, No 2, pp. 1114-1128.

[18] McGrath, B.P.; Holmes, D.G. Multicarrier PWM Strategies for Multilevel Inverters. IEEE Transaction on Industrial Electronics 2002, Volume 49, No. 4, pp. 858-867.

[19] Beristain, J.; Bordonau, J.; Gilabert, A.; Alepuz, S. A new AC/AC multilevel converter for a single-phase inverter with HF isolation. Proceedings IEEE Power Electronics Specialist Conference 2004, Volume 3, pp. 1998–2004.

[20] Jöckel, S.; Herrmann, A.; Rinck, J. High energy production plus built-in reliability–the new Vensys 70/77 gearless wind turbines in the 1.5 MW class. In Proc. European Wind Energy Conf., Athens, Greece 2006.

[21] Kwon, J-M.; Kwon, B-H.; Nam, K-H. Three-phase photovoltaic system with three-level boosting mppt control. IEEE Tran. on Pow. Elec 2008, Volume 23, No 5, pp.2319-2327.

[22] Zhang, M. T.; Jiang, Y.; Lee, F. C.; Jovanovic, M. M. Singlephase three-level boost power factor correction converter. APEC'95 Proc, Volume 1, pp.434-439.

[23] Pinheiro, J. R.; Vidor, D. L. R.; Gründling, H. A.; Dual output three-level boost power factor correction converter with unbalanced loads. Pow. Elec. Spec. Conf., (PESC) 1996, Volume 1, pp.733-729.

[24] Baggio, J. E.; Hey, H. L.; Gründling, H. A.; Pinheiro, H.; Pinheiro, J. R.; Discreate control for three-level boost pfc converter. Int. Tel. Ene. Conf 2002, pp.627-633.

[25] Takagi, M.; Shimizu, K.; Zaitsu, T. Ultra-high efficiency of 95 percent for DC/DC converter - considering theoretical limitation of efficiency APEC. Seventeenth Annual IEEE Applied Power Electronics Conference and Exposition 2002, Volume 2, pp. 735–741.

[26] Ponniran, A.; Orikawa, K.; Itoh, J. i. Modular multi-stage Marx topology for high boost ratio DC/DC converter in HVDC in 2015. IEEE International Telecommunications Energy Conference (INTELEC) 2015, pp. 1–6.

[27] Bin Ponniran, A.; Orikawa, K.; Itoh, J. Fundamental Operation of Marx Topology for High Boost Ratio DCDC Converter. IEEJ J. Ind. Appl 2016, Volume 5, No 4, pp. 329–338.

International Journal of
Electrical and Electronics Research (IJEER)
Research Article | Volume 12, Issue 1 | Pages 178-186 | e-ISSN: 2347-470X

[28] Ponniran, A. B.; Orikawa, K.; Itoh, J. Minimum flying capacitor for N-level capacitor DC/DC boost converter. IEEE Transactions on Industry Applications 2016, Volume 52, No 4, pp.3255-3266.

[29] Rahavi, J. S. A.; Kanagapriya, T.; Seyezhai, R. Design and analysis of Interleaved Boost Converter for renewable energy source2012 International Conference on Computing. Electronics and Electrical Technologies (ICCEET) 2012, pp. 447–451.

[30] Nandankar, P.; Rothe, J. P. Design and implementation of efficient three-phase interleaved DC-DC converter. In International Conference & Workshop on Electronics & Telecommunication Engineering (ICWET 2016) 2016, pp. 1-7.